


# Regional cerebral blood flow estimated by early PiB uptake is reduced in mild cognitive impairment and associated with age in an amyloid-dependent manner

## Journal Article

### Author(s):

Gietl, Anton F.; Warnock, Geoffrey; Riese, Florian; Kälin, Andrea M.; Saake, Antje; Gruber, Esmeralda; Leh, Sandra E.; Unschuld, Paul G.; Kuhn, Felix P.; Burger, Cyrill; [Mu, Linjing](#) ; Seifert, Burkhardt; Nitsch, Roger M.; Schibli, Roger; Ametamey, Simon M.; Buck, Alfred; Hock, Christoph

### Publication date:

2015-04

### Permanent link:

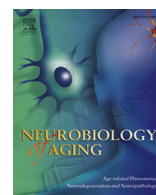
<https://doi.org/10.3929/ethz-b-000100052>

### Rights / license:

[Creative Commons Attribution-NonCommercial-NoDerivatives 4.0 International](#)

### Originally published in:

Neurobiology of Aging 36(4), <https://doi.org/10.1016/j.neurobiolaging.2014.12.036>



## Regional cerebral blood flow estimated by early PiB uptake is reduced in mild cognitive impairment and associated with age in an amyloid-dependent manner



Anton F. Gietl<sup>a,\*</sup>, Geoffrey Warnock<sup>b</sup>, Florian Riese<sup>a</sup>, Andrea M. Kälin<sup>a</sup>, Antje Saake<sup>a</sup>, Esmeralda Gruber<sup>a</sup>, Sandra E. Leh<sup>a</sup>, Paul G. Unschuld<sup>a</sup>, Felix P. Kuhn<sup>b</sup>, Cyrill Burger<sup>b,c</sup>, Linjing Mu<sup>d,e</sup>, Burkhardt Seifert<sup>f</sup>, Roger M. Nitsch<sup>a</sup>, Roger Schibli<sup>d,e</sup>, Simon M. Ametamey<sup>e</sup>, Alfred Buck<sup>b</sup>, Christoph Hock<sup>a</sup>

<sup>a</sup> Division of Psychiatry Research and Psychogeriatric Medicine, University of Zurich, Zurich, Switzerland

<sup>b</sup> Department of Nuclear Medicine, University Hospital Zurich, Zurich, Switzerland

<sup>c</sup> PMOD Technologies Ltd, Zurich, Switzerland

<sup>d</sup> Department of Nuclear Medicine, Center for Radiopharmaceutical Sciences of ETH-PSI-USZ, University Hospital Zurich, Zurich, Switzerland

<sup>e</sup> Department of Chemistry and Applied Biosciences, Center for Radiopharmaceutical Sciences of ETH-PSI-USZ, Institute of Pharmaceutical Sciences, ETH Zurich, Zurich, Switzerland

<sup>f</sup> Department of Biostatistics, Epidemiology, Biostatistics and Prevention Institute, University of Zurich, Zurich, Switzerland

### ARTICLE INFO

#### Article history:

Received 3 November 2013

Received in revised form 22 December 2014

Accepted 26 December 2014

Available online 7 January 2015

#### Keywords:

Alzheimer's disease

Biomarker

MCI

PiB

Amyloid

Cerebral blood flow

PET

Hippocampus

Posterior cingulate cortex

Frontal

MRI

Aging

### ABSTRACT

Early uptake of [<sup>11</sup>C]-Pittsburgh Compound B (ePiB, 0–6 minutes) estimates cerebral blood flow. We studied ePiB in 13 PiB-negative and 10 PiB-positive subjects with mild cognitive impairment (MCI, *n* = 23) and 11 PiB-positive and 74 PiB-negative cognitively healthy elderly control subjects (HCS, *n* = 85) in 6 bilateral volumes of interest: posterior cingulate cortex (PCC), hippocampus (hipp), temporoparietal region, superior parietal gyrus, parahippocampal gyrus (parahipp), and inferior frontal gyrus (IFG) for the associations with cognitive status, age, amyloid deposition, and apolipoprotein E ε4-allele. We observed no difference in ePiB between PiB-positive and -negative subjects and carriers and noncarriers. ePiB decreased with age in PiB-positive subjects in bilateral superior parietal gyrus, bilateral temporoparietal region, right IFG, right PCC, and left parahippocampal gyrus but not in PiB-negative subjects. MCI had lower ePiB than HCS (left PCC, left IFG, and left and right hipp). Lowest ePiB values were found in MCI of 70 years and older, who also displayed high cortical PiB binding. This suggests that lowered regional cerebral blood flow indicated by ePiB is associated with age in the presence but not in the absence of amyloid pathology.

© 2015 The Authors. Published by Elsevier Inc. This is an open access article under the CC BY-NC-ND license (<http://creativecommons.org/licenses/by-nc-nd/4.0/>).

## 1. Introduction

### 1.1. The potential of [<sup>11</sup>C]-Pittsburgh Compound B as a dual biomarker

In the recommendations from the National Institute on Aging-Alzheimer's Association workgroups on the diagnostic guidelines for identifying preclinical Alzheimer's disease (AD) or mild cognitive

impairment (MCI) because of AD, amyloid PET with the [<sup>11</sup>C]-Pittsburgh Compound B (PiB) is considered to be a marker of cerebral amyloid deposition, whereas a reduction in temporoparietal glucose metabolism assessed by [<sup>18</sup>F] fluorodeoxyglucose-positron emission tomography (FDG-PET) is considered a marker of downstream neuronal injury (Albert et al., 2011; Sperling et al., 2011). The same criteria imply that the combination of markers for amyloid deposition, neuronal injury, and synaptic dysfunction is important for the prognosis in MCI and preclinical AD. However, a combination of amyloid- and FDG-PET may not always be feasible because of the higher cost, associated patient discomfort, and radioactive dose burden. In this context, dynamic PET with PiB may be able to provide information on regional cerebral blood flow (rCBF) in addition to the

\* Corresponding author at: Division of Psychiatry Research and Psychogeriatric Medicine, University of Zurich, Wagistr. 12, 8952 Schlieren, Switzerland. Tel.: +41 44 634 9151; fax: +41 79 253 23 88.

E-mail address: [anton.gietl@bli.uzh.ch](mailto:anton.gietl@bli.uzh.ch) (A.F. Gietl).

information on amyloid deposition. Using kinetic modeling, the rate constant K1 for PiB uptake and tracer extraction, which is directly related to CBF, was investigated as an estimate for cortical blood flow. In a rhesus monkey, the regional distributions of K1 and CBF were similar, and changes in K1 were found to closely follow changes in CBF as measured by H<sub>2</sub><sup>15</sup>O PET after increasing the level of CO<sub>2</sub> in the blood (Blomquist et al., 2008). The same study found that PiB K1 was lower in subjects with AD compared with HCS, indicative of lower CBF in AD subjects. Although the exact mechanisms are still under debate, CBF and cerebral glucose metabolism are tightly coupled (Paulson et al., 2010). The correlation between initial PiB uptake in dynamic PET as an estimate of K1 and cerebral glucose metabolism assessed with FDG-PET was studied in a large cohort of subjects with frontotemporal lobe dementia and AD (Rostomian et al., 2011). A time frame for early PiB uptake (1–8 minutes) exhibited a high correlation with FDG uptake and resulted in a comparable diagnostic value for discriminating between AD and frontotemporal lobe dementia. Furthermore, a strong correlation between FDG-PET and early PiB signal using the first 6 minutes of a dynamic PiB-PET scan was shown (Forsberg et al., 2012). When AD, MCI, and HCS were pooled and stratified into PiB-positive and -negative subjects, PiB-positive (i.e., high cortical amyloid load) subjects exhibited lower cerebral glucose metabolism and reduced early uptake of PiB (ePiB) indicating reduced CBF. Correspondingly, relative tracer delivery derived from a simplified reference tissue model has also been demonstrated to be positively correlated with the performance in the Mini-Mental State Examination (Meyer et al., 2011) in brain regions including the bilateral posterior cingulate cortex (PCC)/precuneus, lateral inferior temporal cortex, and temporoparietal junction.

We hypothesized that ePiB, estimating changes in CBF and being correlated with FDG-PET information, would be reduced in patients with MCI compared with healthy elderly control subjects (HCS). We used a maximum probability atlas (Gousias et al., 2008; Hammers et al., 2003) to measure ePiB and amyloid load (PiB uptake between 50 and 70 minutes after tracer injection) in predefined volumes of interest (VOIs). These VOIs cover brain structures with reduced FDG-PET signal described in a recent meta-analysis to be predictive for short-term conversion from MCI to AD (Zhang et al., 2012), namely the temporoparietal cortices (Anchisi et al., 2005; Arnaiz et al., 2001; Chetelat et al., 2003; Drzezga et al., 2005; Landau et al., 2010; Mosconi et al., 2004), PCC (Anchisi et al., 2005; Drzezga et al., 2005; Landau et al., 2010; Nobili et al., 2008), lateral frontal cortex (Nobili et al., 2008), and medi-otemporal structures (Anchisi et al., 2005).

## 1.2. Risk factors of AD and CBF

The aggregation of protein structures (beta-amyloid and tau) is considered as a central feature and an early event in the pathogenesis of AD (Hardy and Higgins, 1992; Jack et al., 2013) that may start decades before the onset of cognitive impairment (Braak et al., 2011; Villemagne et al., 2013) and may affect brain integrity early (Schreiner et al., 2014; Sperling et al., 2009; Steininger et al., 2014). At the time cognitive symptoms become overt, a large number of synaptic connections has already been lost (Arendt, 2009; Scheff et al., 2011), and neurodegeneration can be observed (Mufson et al., 2000). Hypometabolism and also reductions in CBF have been considered to reflect synaptic loss (Giovacchini et al., 2011; Herholz, 2011) and in a broader context neuronal injury. In the hypothesis of the amyloid cascade and in a recently formulated hypothetical biomarker model, they were put downstream to amyloid and tau deposition (Jack et al., 2010). However, studies in subjects at risk of AD, for example, young ApoE4 carriers (Reiman et al., 2004; Scarmeas et al., 2003; Wierenga et al., 2013) or subjects with a family history of AD (Mosconi et al., 2014), have

revealed alterations in glucose metabolism and CBF. Thus, a very early and causative effect might be possible. Few studies on CBF or regional glucose metabolism had also information on amyloid deposition and apolipoprotein E (ApoE) genotype. Lower CBF was identified by arterial spin labeling (ASL) in PiB-positive late MCI and AD (Mattsson et al., 2014). Lower FDG-PET signal indicated hypo-metabolism in cognitively normal apolipoprotein E  $\epsilon$ 4-allele carriers (ApoE4-carriers) compared with noncarriers (Knopman et al., 2014) or in subjects with higher versus lower amyloid load (Knopman et al., 2014; Lowe et al., 2014). In our study, we took advantage of ePiB to study rCBF in addition to cerebral amyloid deposition and ApoE genotype, in subjects who cover a spectrum of cognitively healthy aging and MCI. We addressed potential effects of age, ApoE genotype (ApoE4 carrier vs. noncarrier), and amyloid deposition on rCBF estimated by ePiB.

## 2. Methods

### 2.1. Participants

A total of 25 subjects with MCI and 93 cognitively HCS underwent PET imaging with PiB. Subjects participated in 2 ongoing longitudinal studies and were recruited through regular referrals to the institution's memory clinic, advertisement, and from a preexisting longitudinal cohort. The 93 HCS were recruited from the study "Imaging Brain Beta-Amyloid in Asymptomatic Elderly Subjects." For inclusion, subjects had to be aged between 55 and 80 years. Cognitive health was ascertained by a Mini-Mental State Examination (MMSE) score of  $\geq 27$  and clinical examination that included clinical workup and neuropsychological testing (see also Riese et al., 2015; Steininger et al., 2014). Exclusion criteria were as follows: significant medication or drug abuse that may affect cognition, magnetic resonance imaging (MRI) exclusion criteria, contraindications against venipuncture, clinically relevant changes in red blood cell count, allergy to PiB or any of its constituents, history of severe allergic reactions to drugs or allergens, critical or medically unstable illness, pregnancy or lactation, and significant exposure to radiation. The 25 MCI subjects represent a subgroup from the study "The Conversion of Mild Cognitive Impairment to Alzheimer's Disease." MCI was diagnosed according to the standard criteria (Winblad et al., 2004) after a comprehensive clinical and neuropsychological workup. Subjects had to be of age  $\geq 60$ . Exclusion criteria were as follows: clinically significant neurologic, psychiatric, or internal disease or medication or drug abuse that may affect cognition; clinically significant depression; MRI scans with the evidence of infection, infarction, or other focal lesions; multiple lacunes or lacunes in a critical memory structure; MRI exclusion criteria; contraindications against venipuncture; clinically relevant changes in red blood cell count; exclusion criteria for PiB-PET (as mentioned earlier); and critical or medically unstable illness. Both studies were approved by the cantonal ethics committee of canton Zurich, Switzerland. Subjects were only accepted after providing the written informed consent.

### 2.2. PiB synthesis

Carbon-11 was produced via the  $^{14}\text{N}(p,\alpha)^{11}\text{C}$  nuclear reaction in an on-site cyclotron (16.5 MeV, GE) in the form of [ $^{11}\text{C}$ ]-CO<sub>2</sub>. [ $^{11}\text{C}$ ]-Methyl iodide ([ $^{11}\text{C}$ ]-CH<sub>3</sub>I) was generated in a 2-step reaction sequence involving the catalytic reduction of [ $^{11}\text{C}$ ]CO<sub>2</sub> to [ $^{11}\text{C}$ ]methane and subsequent gas-phase iodination. After passing through an AgOTf/C column at 190 °C, the more reactive [ $^{11}\text{C}$ ]-methyl triflate was formed. PiB was prepared based on the published radiolabeling procedure in a 1-step reaction by reacting the free amine precursor 6-HO-BTA-0 with [ $^{11}\text{C}$ ]-methyl triflate

(Solbach et al., 2005). PiB (approximately 2–4 GBq) was obtained in 99% radiochemical purity after semi-high-performance liquid chromatography purification. The total radiolabeling time was around 40 minutes after the end of bombardment. Specific activity was high and ranged from 80 to 320 GBq/ $\mu\text{mol}$  at the end of the synthesis. The radiochemical yield was 20%–30% (decay corrected). PiB was formulated in saline with <10% ethanol for intravenous injection, and pH was adjusted to 5–6.

### 2.3. PET acquisition

PET acquisition has been published before (Riese et al., 2015; Steininger et al., 2014). An antecubital venous line was positioned for the application of approximately 350 MBq of PiB. Dynamic PET data were acquired for 70 minutes ( $4 \times 15, 8 \times 30, 9 \times 60, 2 \times 180$ , and  $10 \times 300$  seconds). If dynamic scanning was not feasible (e.g., participant incapable of lying still >70 minutes and limited scanner availability), a static image covering 50–70 minutes after tracer injection was acquired for the assessment of cerebral amyloid deposition.

### 2.4. MR acquisition

MCI subjects were scanned on a 1.5-T Phillips Achieva with a sequence repetition time 8.1 ms, echo time 3.7 ms, and  $8^\circ$  flip angle, and field of view for the 160 sagittal slices with 1-mm single-slice thickness was 240 mm anterior-posterior (AP), 240 mm foot to head (FH), and 160 mm right-left (RL). HCS subjects were scanned on a 3-T Phillips Achieva with a repetition time 8.2 ms, echo time 3.7 ms, and  $8^\circ$  flip angle, and field of view for the 220 axial slices with 1-mm single-slice thickness was 240 mm (AP), 220 mm (FH), and 188 mm (RL). Nine MCI subjects were imaged on both the scanners to study a potential effect of scanner on image analysis as MRI is used for coregistration and gray-matter (GM) segmentation. Higher ePiB signal (95% confidence interval [CI] of mean difference not including 0) was observed via the 1.5-T image (MCI)-based analysis pipeline in the right inferior frontal gyrus (IFG), right PCC, right and left hippocampus (hipp), bilateral superior parietal gyrus (SPG), and bilateral temporoparietal region (TR) (Supplementary Table 1).

### 2.5. Image analyses

All image processing was performed using the PMOD PNEURO tool, version 3.4 (PMOD Ltd, Zurich, Switzerland). Frames 1–13 were averaged to aid coregistration with the subject's 3-dimensional T1-weighted MR image using a normalized mutual-information-based registration. After normalization, a maximum probability atlas (Hammers N30R83) was used to define VOIs based on the segmentation of GM and white matter. Segmentation was performed on the individual MRI (50% GM probability). The construction of the N30R83 atlas and the segmentation algorithm have been described elsewhere (Gousias et al., 2008; Hammers et al., 2003). The combined transformation matrices (PET to MR and MR to Montreal Neurologic Institute [MNI] space) were applied to the dynamic PET images to perform all further analyses in the MNI space. The average tracer uptake between 0–6 and 50–70 minutes was calculated from the time-activity curves of the segmented GM VOIs using SAS (version 9.3; SAS Institute Inc, Cary, NC, USA).

### 2.6. Calculation of cortical PiB retention and definition of PiB status cutoff

Mean PiB uptake in all cortical VOIs (excluding occipital lobe, insula, primary motor and sensorimotor cortices) and cerebellar regions was calculated from frames 50–70 minutes using a volume-weighted averaging procedure for derivation of global cortical and

cerebellar PiB uptake, and the cortical-to-cerebellar standardized uptake value ratio was calculated (henceforth “cortical PiB retention” or “PiB retention”). A numerical cutoff to define PiB-positive status was calculated from the entire HCS cohort ( $n = 93$ ) according to a previously described method (Vandenberghe et al., 2010). The resulting cutoff was 1.265.

### 2.7. Calculation of ePiB signal

Average uptake from the first 13 PET frames (0–6 minutes) was standardized by dividing the signal in the respective VOI by the cerebellar mean for the first 0–6 minutes. Regions analyzed for ePiB were single VOIs of the Hammers N30R83: left and right IFG, PCC, hipp, parahippocampal gyrus (parahipp) (including ambient gyrus), SPG, and a volume-weighted averaged group consisting of posterior temporal lobe and inferolateral remainder of parietal lobe henceforth referred to as the TR. Frames 0–6 minutes were selected as they have been shown to correlate with K1 and cerebral glucose metabolism (Forsberg et al., 2012).

### 2.8. ApoE genotyping

ApoE genotyping was performed by the restriction isotyping as previously described (Hixson and Vernier, 1990).

### 2.9. Statistical analyses

Analyses were performed with SPSS 19.0 (SPSS Inc, Chicago, IL, USA) or SAS (version 9.3; SAS Institute Inc, Cary, NC, USA). Outliers were kept in the analysis. Levene test was applied to test homogeneity of variances and Shapiro-Wilk test to test normal distribution. If Shapiro-Wilk test was significant, parametric testing was still considered appropriate if the skewness value was between  $-1$  and  $+1$ . Chi-square tests were applied to test for the association between categorical variables. Spearman rank correlation was used to test for correlations. A correlation ( $\rho$ ) was considered weak between 0.1 to 0.35, moderate between 0.36 and 0.65, and strong  $>0.66$  (the corresponding negative values were used for negative correlations), and  $t$  tests or their respective nonparametric equivalent (Mann-Whitney  $U$  test) were used for group comparisons. Alpha error rate was controlled using the Bonferroni-Holm method (Holm, 1979). Repeated-measures analysis of variance (ANOVA) was used to examine between-subject effects (MCI/HCS: PiB positive/PiB negative and ApoE4 carriers vs. noncarriers). For group comparisons of  $>2$  groups, ANOVA was followed by Fisher least significance difference test with Bonferroni correction for planned comparisons. We conducted 2 subsets of analyses. One focused on the comparison of PiB-positive versus PiB-negative subjects and ApoE4 carriers versus noncarriers, which reflects the biological aspect of cerebral amyloid deposition. The other subset focused on the comparison between MCI and HCS that reflects the clinical aspect of cognitively healthy versus cognitively impaired. For group comparisons, effect sizes were calculated according to  $d = \frac{m_2 - m_1}{SD \text{ pooled}}$ , where standard deviation (SD) pooled was calculated according to

$$SD \text{ pooled} = \sqrt{\frac{(n_2 - 1)SD_2^2 + (n_1 - 1)SD_1^2}{n_1 + n_2 - 2}}$$
 with  $m_2$ ,  $n_2$ , and  $SD_2$  representing mean, sample size, and SD of MCI and  $m_1$ ,  $n_1$ , and  $SD_1$  for HCS. Bias correction was included as follows:  $d_{unbiased} = d \left[ 1 - \frac{3}{4(n_1 + n_2 - 2) - 1} \right]$ . A 95% CI for effect size was calculated as follows: lower limit =  $d - 1.96 \times \text{standard error (SE) of } d$ ; upper limit =  $d + 1.96 \times \text{SE of } d$ . The SE of  $d$  was calculated according to  $dSE = \sqrt{\frac{m_1 + n_2}{n_1 n_2} + \frac{d^2}{2(n_1 + n_2 - 2)}}$ . For calculation of effect sizes, see also formulae 1, 2, 14, 15, and 17 in Nakagawa and Cuthill (2007).



**Table 1**  
Sample description

	<i>n</i>	Age	MMSE	Education	ApoE4 carrier
Total	108	69.2 (6.2)	29.2 (1.2)	15 (2.8)	33 (31%) <sup>a</sup>
HCS/MCI	85/23	68.3 (5.7)/72.3(7.3)	29.5 (0.8)/28.1 (2.0)	15.1 (2.7)/15.0 (2.9)	23/10
PiB positive	21 (19%)	73.1 (6.2)	28.2 (2.1)	14.1 (2.3)	16 (80%) <sup>a</sup>
HCS/MCI	11/10	72.1 (5.7)/74.2 (6.8)	29.5 (0.8)/26.8 (2.2)	14.6 (2.4)/13.4 (2.2)	7/9
PiB negative	87 (81%)	68.2 (5.9)	29.4 (0.8)	15.3 (2.8)	17 (20%) <sup>a</sup>
HCS/MCI	74/13	67.7 (5.5)/70.9 (7.5)	29.5 (0.7)/29.2 (1.1)	15.1 (2.8)/16.2 (2.9)	16/1

Mean and standard deviation (in brackets) are provided for age, MMSE, and education.

Key: ApoE4, apolipoprotein E ε4; HCS, healthy elderly control subjects; MCI, mild cognitive impairment; MMSE, Mini-Mental State Examination; PiB, [<sup>11</sup>C]-Pittsburgh Compound B.

<sup>a</sup> Data on ApoE genotype were missing for 1 PiB-positive and 1 PiB-negative HCS.

### 3. Results

#### 3.1. Sample description

A histogram of cortical PiB retention for the entire sample is presented in [Supplementary Fig. 1](#). ePiB data were available for 108 subjects who were considered for the subsequent analyses. PiB-positive subjects were older than PiB-negative subjects ( $t = -3.4$ , degrees of freedom [df] = 106,  $p < 0.001$ ) and scored lower on the MMSE ( $U = 560.5$ ,  $p = 0.003$ ). MCI were older than HCS ( $t = -2.9$ ,  $df = 106$ ,  $p = 0.005$ ) and scored lower on the MMSE ( $U = 537$ ,  $p < 0.001$ ). [Table 1](#) provides the sample description. ApoE4-carrier status was associated with PiB status ( $\chi^2 = 27.5$ ,  $p < 0.001$ ,  $\phi = 0.51$ ) but not with diagnosis. The odds ratio for an ApoE4 carrier to be PiB positive was 16 (95% CI = 5–55) compared with a noncarrier. Left and right TRs ( $\rho = 0.94$ ,  $p < 0.001$ ) and left and right SPG ( $\rho = 0.93$ ,  $p < 0.001$ ) were strongly correlated and, therefore, averaged to provide a bilateral measure (bilateral SPG and bilateral TR). All other regions were considered separately.

#### 3.2. Influence of amyloid deposition and ApoE4-carrier status on ePiB

Levene test was significant in the left IFG in the right and left hipp and in the TR. Variances (max = 0.005) and variance differences (max = 0.002) were small. We considered repeated-measures ANOVA still appropriate to test the hypothesis that ePiB signal measured in different regions (within-subject factor) demonstrates a mean difference between PiB-positive and -negative subjects (between-subject factor). No differences between PiB-positive and -negative subjects were found ( $p = 0.93$ ). Repeated-measures ANOVA to test for a mean difference between ApoE4 carriers and noncarriers was also not significant ( $p = 0.45$ ).

Scatterplots of PiB retention and ePiB ([Supplementary Fig. 2](#)) did not show a monotonic relationship. This precluded Spearman rank correlation for the entire sample; so, we computed correlations in PiB-positive and -negative subjects separately. No regional association was observed in PiB-positive subjects; however, a moderate positive association was found in the PiB-negative subjects in the bilateral SPG ( $\rho = 0.6$ ,  $p < 0.001$ ).

#### 3.3. Effects of region volume and age on ePiB

The gray-matter VOIs in MNI space and ePiB signal were weak to moderately correlated to ePiB (all adjusted  $p$  values < 0.01) in all regions except the left and right parahipp. In the entire sample, there was a significant negative correlation of ePiB with age in the left hipp ( $\rho = -0.3$ ). When PiB-positive individuals were considered separately, significant correlations were found in the bilateral SPG, bilateral TR, right PCC, left parahipp, and right IFG. Scatterplots of ePiB and age for these regions are provided in [Fig. 1](#). In all other

regions, we observed a negative correlation (see [Table 2](#)), which was not significant after  $p$ -value adjustment. In PiB-negative individuals, no association of ePiB and age was observed. [Table 2](#) reports the associations of ePiB with age for the entire sample and for the PiB-positive and -negative subgroups. In a next step, we examined the association of ePiB with age in ApoE4 carriers and noncarriers separately. No significant difference was found.

#### 3.4. ePiB in MCI versus HCS

Repeated-measures ANOVA was designed to test if ePiB measured in different regions demonstrates a mean difference between MCI and HCS. The assumption of sphericity was violated (Mauchly test of sphericity:  $f = 391$ ,  $p < 0.001$ ); therefore, a Greenhouse-Geisser correction was applied ( $\epsilon = 0.518$ ). A significant difference was observed in ePiB for the different regions (within-subject effects) ( $df = 4.66$ ,  $F = 999$ ,  $p < 0.001$ ). There was an interaction between region and diagnosis ( $df = 4.66$ ,  $F = 3.63$ ,  $p = 0.004$ ) and a significant mean reduction in ePiB in MCI compared with HCS (between-subject effects) ( $df = 1$ ,  $F = 7.33$ ,  $p = 0.008$ ). Regions with significant lower ePiB ( $p$  values surviving Bonferroni-Holm correction for 10 comparisons) included the left PCC ( $d = -0.8$ , 95% CI =  $-1.3$  to  $-0.3$ ,  $p < 0.001$ ), left hipp ( $d = -0.8$ , 95% CI =  $-1.3$  to  $-0.3$ ,  $p < 0.001$ ), right ( $d = -0.9$ , 95% CI =  $-1.4$  to  $-0.4$ ,  $p = 0.004$ ) hipp, and left IFG ( $d = -0.8$ , 95% CI =  $-1.3$  to  $-0.3$ ,  $p < 0.001$ ). To account for the potential influence of age and PiB status on ePiB, we introduced an age split at 70 years and conducted a first ANOVA which demonstrated that ePiB differed between young HCS, young MCI, old HCS, and old MCI ( $df = 3$ , 104,  $p < 0.001$  for left and right hipp,  $p < 0.01$  for left IFG and PCC). No significant mean differences were found for planned comparison between the young subjects. Planned comparison between old HCS and old MCI revealed strong reductions in ePiB in the all the regions as displayed on the boxplots in [Fig. 2A](#). Effect sizes and corrected  $p$  values (2 comparisons) were as follows: left IFG ( $d = -0.9$ , 95% CI =  $-1.5$  to  $-0.3$ ,  $p = 0.021$ ), left PCC ( $d = -1.0$ , 95% CI =  $-1.7$  to  $-0.4$ ,  $p < 0.001$ ), left hipp ( $d = -1.2$ , 95% CI =  $-1.8$  to  $-0.5$ ,  $p < 0.001$ ), and right hipp ( $d = -1.4$ , 95% CI =  $-2.1$  to  $-0.7$ ,  $p < 0.001$ ). In a second ANOVA to account for PiB status, ePiB signal differed between young HCS, old HCS, young PiB-positive MCI, young PiB-negative MCI, old PiB-positive MCI, and old PiB-negative MCI ( $df = 5$ , 102,  $p < 0.001$  for left and right hipp,  $p < 0.05$  for left IFG and left PCC). The first planned comparison old HCS versus old PiB-negative MCI demonstrated a reduction in the right hipp for MCI ( $d = -1.3$ , 95% CI =  $-2.1$  to  $-0.4$ ) and the second planned comparison old HCS versus old PiB-positive MCI identified lower ePiB in the left IFG ( $d = -1.2$ , 95% CI =  $-2.0$  to  $-0.3$ ,  $p = 0.02$ ), left PCC ( $d = -1.2$ , 95% CI =  $-2.1$  to  $-0.4$ ,  $p = 0.002$ ), left hipp ( $d = -1.9$ , 95% CI =  $-2.9$  to  $-1$ ,  $p < 0.001$ ) and right hipp ( $d = -1.7$ , 95% CI =  $-2.6$  to  $-0.8$ ,  $p < 0.001$ ). These comparisons are displayed in [Fig. 2B](#).

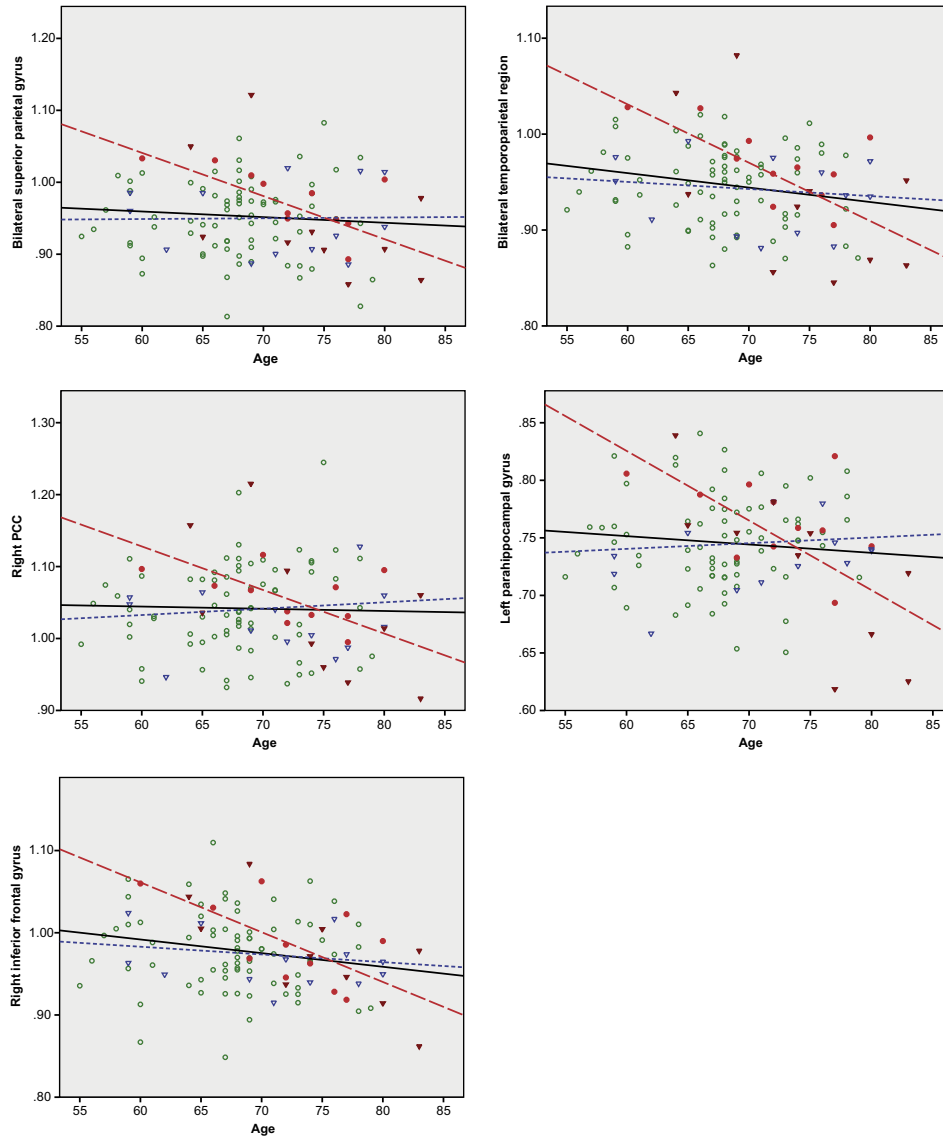


**Fig. 1.** Scatterplots of age (x axis) and early uptake of [<sup>11</sup>C]-Pittsburgh Compound B (ePiB) (y axis). ePiB is inversely correlated with age in PiB-positive individuals (fit line: long dashes, red; mild cognitive impairment [MCI]: filled triangles, dark red; and HCS: filled circles, light red) not in PiB-negative individuals (fit line: short dashes, blue; MCI: empty triangles, blue; and HCS, empty circles, green). The black continuous line represents the fit line for the entire sample.

**4. Discussion**

To our knowledge, this is the first study to investigate ePiB signal as an estimate of rCBF in a large number of subjects with MCI and

HCS. We demonstrate a negative correlation of the rCBF estimate ePiB with age in amyloid-positive individuals but not in amyloid-negative individuals in regions relevant for AD. Furthermore, our study is the first to demonstrate that ePiB identifies reduced rCBF in

**Table 2**  
Correlation of ePiB with age

	Left inf. frontal	Right inf frontal	Left PCC	Right PCC	Left parahipp	Right parahipp	Left hipp	Right hipp	Bilat sup parietal	Bilat temporoparietal
All	-0.25 <i>p</i> = 0.010	-0.23 <i>p</i> = 0.019	-0.14 <i>p</i> = 0.142	-0.03 <i>p</i> = 0.759	-0.02 <i>p</i> = 0.804	-0.09 <i>p</i> = 0.370	<b>-0.30</b> <i>p</i> = <b>0.002*</b>	-0.22 <i>p</i> = 0.021	-0.09 <i>p</i> = 0.372	-0.19 <i>p</i> = 0.056
PiB positive	-0.46 <i>p</i> = 0.038	<b>-0.63</b> <i>p</i> = <b>0.003*</b>	-0.35 <i>p</i> = 0.124	<b>-0.59</b> <i>p</i> = <b>0.005*</b>	<b>-0.66</b> <i>p</i> = <b>0.001*</b>	-0.47 <i>p</i> = 0.033	-0.50 <i>p</i> = 0.021	-0.49 <i>p</i> = 0.025	<b>-0.61</b> <i>p</i> = <b>0.004*</b>	<b>-0.57</b> <i>p</i> = <b>0.007*</b>
PiB negative	-0.16 <i>p</i> = 0.134	-0.15 <i>p</i> = 0.163	-0.08 <i>p</i> = 0.492	0.07 <i>p</i> = 0.517	0.10 <i>p</i> = 0.341	0.02 <i>p</i> = 0.837	-0.22 <i>p</i> = 0.044	-0.18 <i>p</i> = 0.101	0.01 <i>p</i> = 0.898	-0.10 <i>p</i> = 0.375

Spearman rho is provided for all regions, and *p* values are reported uncorrected. Significant associations after Bonferroni-Holm adjustment for 10 comparisons are marked in bold and with an asterisk.

Key: bilat, bilateral; ePiB, early uptake of [<sup>11</sup>C]-Pittsburgh Compound B; hipp, hippocampus; inf, inferior; parahipp, parahippocampal gyrus; PCC, posterior cingulate cortex; sup, superior.

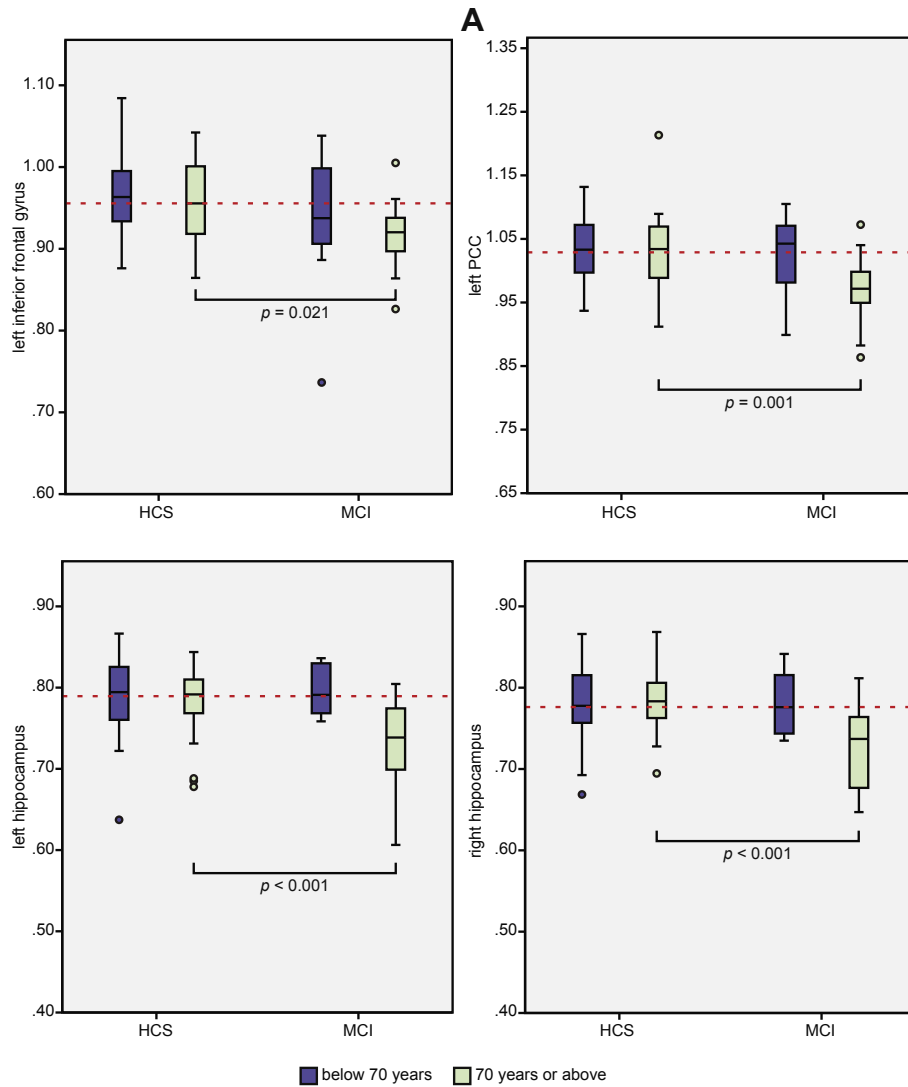


**Fig. 2.** (A) Boxplots of early uptake of [ $^{11}\text{C}$ ]-Pittsburgh Compound B (ePiB) signal (y axis) in regions showing significant reductions in the mild cognitive impairment (MCI) of >70 years of age compared with the HCS of >70 years of age. The dashed red line represents the median of the entire sample. (B) Boxplots of ePiB signal (y axis) for HCS and MCI including PiB status for MCI. The study subjects <70 years are depicted in dark blue and the study subjects >70 years in light green. The dashed line represents the median of the entire sample.

MCI. The effects we found were stronger in older MCI subjects, especially in those who also display elevated amyloid deposition.

#### 4.1. The biological underpinnings of the ePiB signal

The biological relevance of the ePiB signal has been demonstrated in studies that have revealed strong correlations with cerebral glucose metabolism measured by FDG-PET (Forsberg et al., 2012; Fu et al., 2014; Meyer et al., 2011; Rostomian et al., 2011). However, the original concept of assessing ePiB signal is that it estimates cortical blood flow (Blomquist et al., 2008), which is coupled to cerebral glucose metabolism (Paulson et al., 2010). Our own data suggest that volume effects also contribute to ePiB signal in the absence of partial volume correction; however, correlation between volumes and ePiB signal was only weak to moderate. A recent study found that ePiB only approximates CBF because of an average extraction fraction of 0.53; however, relative changes in cortical blood flow between AD patients and controls and relative changes of ePiB signal from the first 1–5 minutes correlated at an  $R^2$  of 0.99 (Gjedde et al., 2013).

#### 4.2. Association of age with ePiB as an estimate of rCBF in PiB-positive subjects

In our study, we observed no mean differences in rCBF estimates between PiB-positive and -negative subjects. ePiB was negatively correlated with age in PiB-positive subjects but not in PiB-negative subjects which is a new finding. An interaction of ApoE4 and age on CBF has been described (Wierenga et al., 2013) that indirectly supports our findings as ApoE4 is the strongest predictor of high amyloid deposition in healthy subjects (Mielke et al., 2012), which we also found in our sample. Hypermetabolism associated with amyloid load has been demonstrated before in cognitively healthy subjects (Oh et al., 2014). Interestingly, 2 studies including individuals from the Mayo Clinic Study of Aging have identified reduced FDG signal in subjects with elevated amyloid deposition (Knopman et al., 2014; Lowe et al., 2014) in regions where we found the age amyloid-status interaction. Of note, in one of these studies, the subjects for studying the association of metabolism and amyloid deposition were older than 70 years and the second included subjects with a median age >77 years. This could be a potential

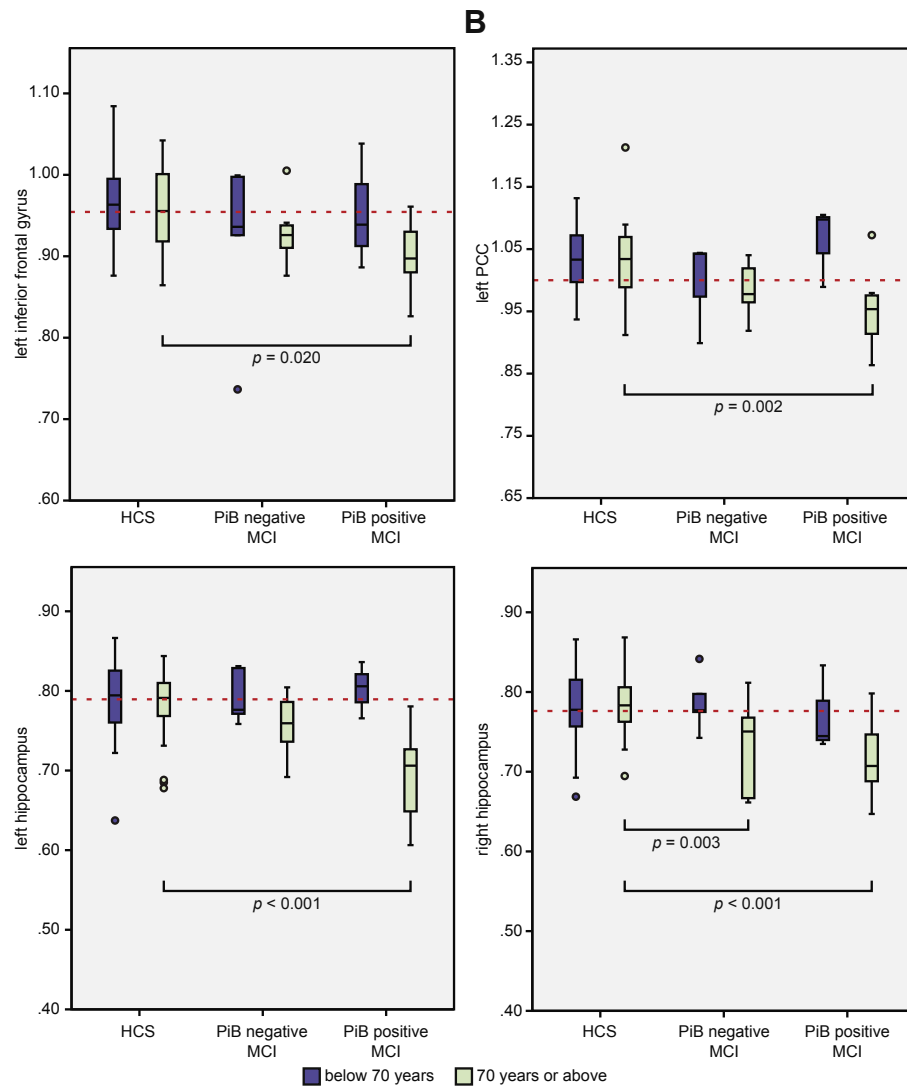


Fig. 2. (continued).

reason that with our younger population, we could observe the interaction but no group differences between PiB-positive and -negative subjects. Furthermore, we did also include subjects with MCI in our analyses to encompass a broader spectrum of the aging population. Several explanations may account for the association of rCBF-estimate ePiB with age in PiB-positive individuals but not in PiB-negative subjects. As suggested by the amyloid hypothesis of AD (Hardy and Higgins, 1992) and the hypothetical model of dynamic biomarkers (Jack et al., 2010, 2013), we first observe amyloid accumulation which as the disease progresses will be accompanied by synaptic loss and neurodegeneration with the consequence of reduced rCBF. Furthermore, our observations are consistent with the evidence of increased metabolism and CBF at some point in the pathogenesis of AD that is later followed by a phase of reduced CBF (Ostergaard et al., 2013; Thambisetty et al., 2010). Hypermetabolism could be a compensatory mechanism (Elman et al., 2014) (Mormino et al., 2012) or simply an indicator of aberrant neuronal activity as a consequence of amyloid deposition (Kellner et al., 2014; Sperling et al., 2009). Conversely, aberrant neuronal activity could promote amyloid deposition (Bero et al., 2011; Cirrito et al., 2005). Important in this context is our finding of the positive association of ePiB and late PiB signal in the superior parietal gyrus in PiB-negative individuals. This could imply a pattern of low-level

amyloid deposition associated with higher rCBF that is disrupted in subjects where high levels of amyloid deposition are reached.

Reductions in CBF with older age in PiB-positive subjects could be caused by a decreasing vascular reserve (Brown and Thore, 2011) or the influence of vascular amyloid deposition (cerebral amyloid angiopathy) that has been implied by pathologic (Thal et al., 2008) and imaging studies in humans (Chung et al., 2009; Peca et al., 2013) and in animal studies (Merlini et al., 2011). A recent article showed that transgenic APP23 mice that are prone to develop plaques and cerebral amyloid angiopathy (Maier et al., 2014) display a loss of cerebral perfusion with increasing age and disease progression, whereas nontransgenic litter mates did not display any change in rCBF. A second mouse model of AD (APPSP1), which is usually devoid of CA, did not show changes in CBF at any age. Translating this to our results suggests that pathologically defined cerebral amyloid angiopathy may contribute to the observed reductions of CBF with age.

Another important aspect of our findings is that in amyloid-negative subjects, we observe no changes between age and the rCBF estimate. Previous studies on the association of CBF with age have shown inconsistent results with some studies finding age-associated decline (Aanerud et al., 2012; Leenders et al., 1990; Marchal et al., 1992) and others not (Meltzer et al., 2000; Takada



et al., 1992). As AD becomes highly prevalent with increasing age, it is difficult to conduct these studies without including subjects that already have evidence of AD (Jagust, 2013). We believe that our PiB-negative subjects with preserved rCBF estimate represent an important phenotype of healthy aging. The remaining question is whether stable rCBF prevents amyloid deposition, which is supported by the fact that vascular risk factors also contribute to the risk of AD (Akinyemi et al., 2013; Hasnain and Victor, 2014), or if rCBF is preserved in the absence of strong amyloid deposition. The first possibility would strongly argue for therapeutic strategies focusing on CBF in the prevention of AD.

#### 4.3. Reduced ePiB in MCI compared with HCS

The regions that we studied were selected under the premise that they were associated with MCI or predictive of cognitive decline in FDG-PET studies as ePiB was linked to FDG-PET in the previous studies (Forsberg et al., 2012; Fu et al., 2014; Meyer et al., 2011; Rostomian et al., 2011). Similar to the FDG-PET studies, we identified reduced rCBF estimates in the left and right hippocampus (De Santi et al., 2001; Li et al., 2008; Mevel et al., 2007; Mosconi et al., 2005; Nestor et al., 2003) and the PCC (Anchisi et al., 2005; Drzezga et al., 2005; Landau et al., 2010; Nobili et al., 2008). When CBF is assessed by ASL, reductions in MCI compared with HCS were also detected in the left PCC, but in the hippocampus, also increases of CBF have been reported (Alsop et al., 2010).

In our sample, no significant reductions in ePiB were found in either the superior parietal gyrus or TR where hypometabolism was described by FDG-PET (Anchisi et al., 2005; Arnaiz et al., 2001; Chetelat et al., 2003; Drzezga et al., 2005; Landau et al., 2010; Mosconi et al., 2004) and ASL literature (Alsop et al., 2010). This may be because of the limited size of our MCI group. In a larger multicentre cohort, hippocampal and PCC hypometabolism was present in 81% of 114 MCI subjects, whereas additional lateral temporal and inferior parietal hypometabolism was only present in 25% of the cases and more frequent in subjects with multiple-domain MCI (Mosconi et al., 2008). We also found a reduction in ePiB in the left inferior frontal cortex. Evidence for the role of this region in MCI/AD is not as abundant as for the regions discussed earlier. A cluster with reduced glucose metabolism has been found in inferior frontal structures when either stable MCI or MCI converters after 1 year were compared with controls (Drzezga et al., 2003). A cluster of hypometabolism in the left IFG was also found in healthy subjects that have declined to MCI (de Leon et al., 2001). ApoE4 carriers that converted from MCI to AD displayed lower median metabolism in the left IFG compared with ApoE4 carriers that did not convert or noncarriers (Mosconi et al., 2004). Our results provide additional evidence for impaired cerebral metabolism or respectively blood flow in the left IFG in MCI. We believe that such an effect is plausible because of this region's involvement in semantic and phonological processing (Costafreda et al., 2006; Katzev et al., 2013), in processes of empathy and working memory (Liakakis et al., 2011), and in tasks of self-awareness (Morin and Michaud, 2007).

#### 4.4. Contributions of age and amyloid status to the reduction of ePiB in MCI

A recent ASL study identified rCBF reductions in AD regions (among others, the hipp) when they compared AD subjects or PiB-positive MCI with amyloid-negative controls but not when they compared CBF in MCI with controls (not considering the amyloid status) (Mattsson et al., 2014). Consistent with that, we found the strongest reductions of ePiB in older MCI cases who are also PiB positive. Therefore, individuals with 3 major risk factors for

Alzheimer's dementia, that is, age, amyloid deposition, and cognitive impairment had the lowest estimates of rCBF. This implies a potential for ePiB in identifying individuals at risk of Alzheimer's dementia.

#### 4.5. Limitations

Our study has some limitations. We included no partial volume correction; so, atrophy could have contributed to the effects of reduced ePiB. We used different MRI scans for MCI and HCS. In MCI, this could have resulted in higher ePiB signals. However, as we observe an effect in the opposite direction, that is, lower ePiB in MCI compared with HCS, we can be sure that this effect is not simply caused by this methodological issue. Our data are cross sectional; so, we cannot truly elaborate on the predictive value of ePiB for cognitive decline. A limitation for interpreting the finding for the association of age and ePiB in PiB-positive subjects is that the ePiB signal is not an absolute measurement of cortical blood flow. Also the PiB-positive subjects were slightly older than the PiB-negative subjects; so, we cannot entirely exclude the possibility that a factor independent of amyloid deposition becomes active on CBF with higher age.

### 5. Conclusions

ePiB as an estimate for rCBF is associated with risk factors for Alzheimer's dementia. This warrants a longitudinal study on the predictive value of ePiB in comparison with other easily accessible biomarkers, for example, volumetric MR measures or ASL. Our cross-sectional findings suggest an association of rCBF with age in subjects with elevated amyloid deposition but not in subjects with low-level amyloid deposition. This could mean that intact CBF in the absence of amyloid deposition constitutes a phenotype of healthy aging, whereas in the presence of amyloid deposition, a reduction of CBF with age occurs in the context of AD.

#### Disclosure statement

Dr Burger is a shareholder and employee of PMOD Technologies Ltd. Dr Warnock is a consultant for PMOD Technologies Ltd.

#### Acknowledgements

This work was supported by the Swiss National Science Foundation grants 320030\_125378 and 33CM30-124111 and Clinical Research Priority Program Molecular Imaging, University of Zurich. GW was supported by the Clinical Research Priority Program Tumor Oxygenation, University of Zurich. The authors would like to thank Ernst Seiffert, Lena Jellestad, Luka Kulic, Senol Apaydin, and Simon Schreiner for their support of the cohort studies; Wiebke Buck and Diana Bundschuh for the support of ApoE genotyping; and Faith Sieber, Isabella Blum, Sabine Spörri, and Stefan Kluge for study coordination and data management.

#### Appendix A. Supplementary data

Supplementary data associated with this article can be found, in the online version, at <http://dx.doi.org/10.1016/j.neurobiolaging.2014.12.036>.

#### References

Aanerud, J., Borghammer, P., Chakravarty, M.M., Vang, K., Rodell, A.B., Jonsdottir, K.Y., Moller, A., Ashkanian, M., Vafae, M.S., Iversen, P., Johannsen, P., Gjedde, A.,

2012. Brain energy metabolism and blood flow differences in healthy aging. *J. Cereb. Blood Flow Metab.* 32, 1177–1187.
- Akinyemi, R.O., Muktaetova-Ladinska, E.B., Attems, J., Ihara, M., Kalaria, R.N., 2013. Vascular risk factors and neurodegeneration in ageing related dementias: Alzheimer's disease and vascular dementia. *Curr. Alzheimer Res.* 10, 642–653.
- Albert, M.S., DeKosky, S.T., Dickson, D., Dubois, B., Feldman, H.H., Fox, N.C., Gamst, A., Holtzman, D.M., Jagust, W.J., Petersen, R.C., Snyder, P.J., Carrillo, M.C., Thies, B., Phelps, C.H., 2011. The diagnosis of mild cognitive impairment due to Alzheimer's disease: recommendations from the National Institute on Aging-Alzheimer's Association workgroups on diagnostic guidelines for Alzheimer's disease. *Alzheimers Dement.* 7, 270–279.
- Alsop, D.C., Dai, W., Grossman, M., Detre, J.A., 2010. Arterial spin labeling blood flow MRI: its role in the early characterization of Alzheimer's disease. *J. Alzheimers Dis.* 20, 871–880.
- Anchisi, D., Borroni, B., Franceschi, M., Kerrouche, N., Kalbe, E., Beuthien-Beumann, B., Cappa, S., Lenz, O., Ludecke, S., Marcone, A., Mielke, R., Ortelli, P., Padovani, A., Pelati, O., Pupi, A., Scarpini, E., Weisenbach, S., Herholz, K., Salmon, E., Holthoff, V., Sorbi, S., Fazio, F., Perani, D., 2005. Heterogeneity of brain glucose metabolism in mild cognitive impairment and clinical progression to Alzheimer disease. *Arch. Neurol.* 62, 1728–1733.
- Arendt, T., 2009. Synaptic degeneration in Alzheimer's disease. *Acta Neuropathol.* 118, 167–179.
- Arnaiz, E., Jelic, V., Almkvist, O., Wahlund, L.O., Winblad, B., Valind, S., Nordberg, A., 2001. Impaired cerebral glucose metabolism and cognitive functioning predict deterioration in mild cognitive impairment. *Neuroreport* 12, 851–855.
- Bero, A.W., Yan, P., Roh, J.H., Cirrito, J.R., Stewart, F.R., Raichle, M.E., Lee, J.M., Holtzman, D.M., 2011. Neuronal activity regulates the regional vulnerability to amyloid-beta deposition. *Nat. Neurosci.* 14, 750–756.
- Blomquist, G., Engler, H., Nordberg, A., Ringheim, A., Wall, A., Forsberg, A., Estrada, S., Frandberg, P., Antoni, G., Langstrom, B., 2008. Unidirectional influx and net accumulation of PIB. *Open Neuroimaging J.* 2, 114–125.
- Braak, H., Thal, D.R., Ghebremedhin, E., Del Tredici, K., 2011. Stages of the pathologic process in Alzheimer disease: age categories from 1 to 100 years. *J. Neuropathol. Exp. Neurol.* 70, 960–969.
- Brown, W.R., Thore, C.R., 2011. Review: cerebral microvascular pathology in ageing and neurodegeneration. *Neuropathol. Appl. Neurobiol.* 37, 56–74.
- Chetelat, G., Desgranges, B., de la Sayette, V., Viader, F., Eustache, F., Baron, J.C., 2003. Mild cognitive impairment: can FDG-PET predict who is to rapidly convert to Alzheimer's disease? *Neurology* 60, 1374–1377.
- Chung, Y.A., O, J.H., Kim, J.Y., Kim, K.J., Ahn, K.J., 2009. Hypoperfusion and ischemia in cerebral amyloid angiopathy documented by 99mTc-ECD brain perfusion SPECT. *J. Nucl. Med.* 50, 1969–1974.
- Cirrito, J.R., Yamada, K.A., Finn, M.B., Sloviter, R.S., Bales, K.R., May, P.C., Schoepp, D.D., Paul, S.M., Mennerick, S., Holtzman, D.M., 2005. Synaptic activity regulates interstitial fluid amyloid-beta levels in vivo. *Neuron* 48, 913–922.
- Costafreda, S.G., Fu, C.H., Lee, L., Everitt, B., Brammer, M.J., David, A.S., 2006. A systematic review and quantitative appraisal of fMRI studies of verbal fluency: role of the left inferior frontal gyrus. *Hum. Brain Mapp.* 27, 799–810.
- de Leon, M.J., Convit, A., Wolf, O.T., Tarshish, C.Y., DeSanti, S., Rusinek, H., Tsui, W., Kandil, E., Scherer, A.J., Roche, A., Imossi, A., Thorn, E., Bobinski, M., Caraos, C., Lesbre, P., Schlyer, D., Poirier, J., Reisberg, B., Fowler, J., 2001. Prediction of cognitive decline in normal elderly subjects with 2-[(18)F]fluoro-2-deoxy-D-glucose/positron-emission tomography (FDG/PET). *Proc. Natl. Acad. Sci. U. S. A.* 98, 10966–10971.
- De Santi, S., de Leon, M.J., Rusinek, H., Convit, A., Tarshish, C.Y., Roche, A., Tsui, W.H., Kandil, E., Boppana, M., Daisley, K., Wang, G.J., Schlyer, D., Fowler, J., 2001. Hippocampal formation glucose metabolism and volume losses in MCI and AD. *Neurobiol. Aging* 22, 529–539.
- Drzezga, A., Grimmer, T., Riemenschneider, M., Lautenschlager, N., Siebner, H., Alexopoulos, P., Minoshima, S., Schwaiger, M., Kurz, A., 2005. Prediction of individual clinical outcome in MCI by means of genetic assessment and (18)F-FDG PET. *J. Nucl. Med.* 46, 1625–1632.
- Drzezga, A., Lautenschlager, N., Siebner, H., Riemenschneider, M., Willloch, F., Minoshima, S., Schwaiger, M., Kurz, A., 2003. Cerebral metabolic changes accompanying conversion of mild cognitive impairment into Alzheimer's disease: a PET follow-up study. *Eur. J. Nucl. Med. Mol. Imaging* 30, 1104–1113.
- Elman, J.A., Oh, H., Madison, C.M., Baker, S.L., Vogel, J.W., Marks, S.M., Crowley, S., O'Neil, J.P., Jagust, W.J., 2014. Neural compensation in older people with brain amyloid-beta deposition. *Nat. Neurosci.* 17, 1316–1318.
- Forsberg, A., Engler, H., Blomquist, G., Langstrom, B., Nordberg, A., 2012. The use of PIB-PET as a dual pathological and functional biomarker in AD. *Biochim. Biophys. Acta* 1822, 380–385.
- Fu, L., Liu, L., Zhang, J., Xu, B., Fan, Y., Tian, J., 2014. Comparison of dual-biomarker PIB-PET and dual-tracer PET in AD diagnosis. *Eur. Radiol.* 24, 2800–2809.
- Giovacchini, G., Squitieri, F., Esmailzadeh, M., Milano, A., Mansi, L., Ciarmiello, A., 2011. PET translates neurophysiology into images: a review to stimulate a network between neuroimaging and basic research. *J. Cell. Physiol.* 226, 948–961.
- Gjedde, A., Aanerud, J., Braendgaard, H., Rodell, A.B., 2013. Blood-brain transfer of Pittsburgh compound B in humans. *Front. Aging Neurosci.* 5, 70.
- Gousias, I.S., Rueckert, D., Heckemann, R.A., Dyet, L.E., Boardman, J.P., Edwards, A.D., Hammers, A., 2008. Automatic segmentation of brain MRIs of 2-year-olds into 83 regions of interest. *Neuroimage* 40, 672–684.
- Hammers, A., Allom, R., Koeppe, M.J., Free, S.L., Myers, R., Lemieux, L., Mitchell, T.N., Brooks, D.J., Duncan, J.S., 2003. Three-dimensional maximum probability atlas of the human brain, with particular reference to the temporal lobe. *Hum. Brain Mapp.* 19, 224–247.
- Hardy, J.A., Higgins, G.A., 1992. Alzheimer's disease: the amyloid cascade hypothesis. *Science* 256, 184–185.
- Hasnain, M., Victor, R.V.W., 2014. Possible role of vascular risk factors in Alzheimer's disease and vascular dementia. *Curr. Pharm. Des.* 20, 6007–6013.
- Herholz, K., 2011. Perfusion SPECT and FDG-PET. *Int. Psychogeriatr.* 23 (Suppl 2), S25–S31.
- Hixson, J.E., Vernier, D.T., 1990. Restriction isotyping of human apolipoprotein E by gene amplification and cleavage with HhaI. *J. Lipid Res.* 31, 545–548.
- Holm, S., 1979. A simple sequentially rejective multiple test procedure. *Scand. J. Stat.* 6, 65–70.
- Jack Jr., C.R., Knopman, D.S., Jagust, W.J., Petersen, R.C., Weiner, M.W., Aisen, P.S., Shaw, L.M., Vemuri, P., Wiste, H.J., Weigand, S.D., Lesnick, T.G., Pankratz, V.S., Donohue, M.C., Trojanowski, J.Q., 2013. Tracking pathophysiological processes in Alzheimer's disease: an updated hypothetical model of dynamic biomarkers. *Lancet Neurol.* 12, 207–216.
- Jack Jr., C.R., Knopman, D.S., Jagust, W.J., Shaw, L.M., Aisen, P.S., Weiner, M.W., Petersen, R.C., Trojanowski, J.Q., 2010. Hypothetical model of dynamic biomarkers of the Alzheimer's pathological cascade. *Lancet Neurol.* 9, 119–128.
- Jagust, W., 2013. Vulnerable neural systems and the borderland of brain aging and neurodegeneration. *Neuron* 77, 219–234.
- Katzev, M., Tuscher, O., Hennig, J., Weiller, C., Kaller, C.P., 2013. Revisiting the functional specialization of left inferior frontal gyrus in phonological and semantic fluency: the crucial role of task demands and individual ability. *J. Neurosci.* 33, 7837–7845.
- Kellner, V., Menkes-Caspi, N., Beker, S., Stern, E.A., 2014. Amyloid-beta alters ongoing neuronal activity and excitability in the frontal cortex. *Neurobiol. Aging* 35, 1982–1991.
- Knopman, D.S., Jack Jr., C.R., Wiste, H.J., Lundt, E.S., Weigand, S.D., Vemuri, P., Lowe, V.J., Kantarci, K., Gunter, J.L., Senjem, M.L., Mielke, M.M., Roberts, R.O., Boeve, B.F., Petersen, R.C., 2014. 18F-fluorodeoxyglucose positron emission tomography, aging, and apolipoprotein E genotype in cognitively normal persons. *Neurobiol. Aging* 35, 2096–2106.
- Landau, S.M., Harvey, D., Madison, C.M., Reiman, E.M., Foster, N.L., Aisen, P.S., Petersen, R.C., Shaw, L.M., Trojanowski, J.Q., Jack Jr., C.R., Weiner, M.W., Jagust, W.J., Alzheimer's Disease Neuroimaging Initiative, 2010. Comparing predictors of conversion and decline in mild cognitive impairment. *Neurology* 75, 230–238.
- Leenders, K.L., Perani, D., Lammertsma, A.A., Heather, J.D., Buckingham, P., Healy, M.J., Gibbs, J.M., Wise, R.J., Hatazawa, J., Herold, S., Beaney, R.P., Brooks, D.J., Spinks, T., Rhodes, C., Frackowiak, R.S.J., 1990. Cerebral blood flow, blood volume and oxygen utilization. Normal values and effect of age. *Brain* 113 (Pt 1), 27–47.
- Li, Y., Rinne, J.O., Mosconi, L., Pirraglia, E., Rusinek, H., DeSanti, S., Kempainen, N., Nagren, K., Kim, B.C., Tsui, W., de Leon, M.J., 2008. Regional analysis of FDG and PIB-PET images in normal aging, mild cognitive impairment, and Alzheimer's disease. *Eur. J. Nucl. Med. Mol. Imaging* 35, 2169–2181.
- Liakakis, G., Nickel, J., Seitz, R.J., 2011. Diversity of the inferior frontal gyrus—a meta-analysis of neuroimaging studies. *Behav. Brain Res.* 225, 341–347.
- Lowe, V.J., Weigand, S.D., Senjem, M.L., Vemuri, P., Jordan, L., Kantarci, K., Boeve, B., Jack Jr., C.R., Knopman, D., Petersen, R.C., 2014. Association of hypometabolism and amyloid levels in aging, normal subjects. *Neurology* 82, 1959–1967.
- Maier, F.C., Wehr, H.F., Schmid, A.M., Mannheim, J.G., Wiehr, S., Lerdkrai, C., Calaminus, C., Stahlschmidt, A., Ye, L., Burnet, M., Stiller, D., Sabri, O., Reischl, G., Staufenbiel, M., Garaschuk, O., Jucker, M., Pichler, B.J., 2014. Longitudinal PET-MRI reveals beta-amyloid deposition and rCBF dynamics and connects vascular amyloidosis to quantitative loss of perfusion. *Nat. Med.* 20, 1485–1492.
- Marchal, G., Rioux, P., Petit-Taboue, M.C., Sette, G., Traverre, J.M., Le Poec, C., Courthouex, P., Derlon, J.M., Baron, J.C., 1992. Regional cerebral oxygen consumption, blood flow, and blood volume in healthy human aging. *Arch. Neurol.* 49, 1013–1020.
- Mattsson, N., Tosun, D., Insel, P.S., Simonson, A., Jack Jr., C.R., Beckett, L.A., Donohue, M., Jagust, W., Schuff, N., Weiner, M.W., Alzheimer's Disease Neuroimaging Initiative, 2014. Association of brain amyloid-beta with cerebral perfusion and structure in Alzheimer's disease and mild cognitive impairment. *Brain* 137 (Pt 5), 1550–1561.
- Meltzer, C.C., Cantwell, M.N., Greer, P.J., Ben-Eliezer, D., Smith, G., Frank, G., Kaye, W.H., Houck, P.R., Price, J.C., 2000. Does cerebral blood flow decline in healthy aging? A PET study with partial-volume correction. *J. Nucl. Med.* 41, 1842–1848.
- Merlini, M., Meyer, E.P., Ulmann-Schuler, A., Nitsch, R.M., 2011. Vascular beta-amyloid and early astrocyte alterations impair cerebrovascular function and cerebral metabolism in transgenic arcAbeta mice. *Acta Neuropathol.* 122, 293–311.
- Mevel, K., Desgranges, B., Baron, J.C., Landeau, B., De la Sayette, V., Viader, F., Eustache, F., Chetelat, G., 2007. Detecting hippocampal hypometabolism in mild cognitive impairment using automatic voxel-based approaches. *Neuroimage* 37, 18–25.
- Meyer, P.T., Hellwig, S., Amtage, F., Rotteberger, C., Sahm, U., Reuland, P., Weber, W.A., Hull, M., 2011. Dual-biomarker imaging of regional cerebral amyloid load and neuronal activity in dementia with PET and 11C-labeled Pittsburgh compound B. *J. Nucl. Med.* 52, 393–400.
- Mielke, M.M., Wiste, H.J., Weigand, S.D., Knopman, D.S., Lowe, V.J., Roberts, R.O., Geda, Y.E., Swenson-Dravis, D.M., Boeve, B.F., Senjem, M.L., Vemuri, P.,

- Petersen, R.C., Jack Jr., C.R., 2012. Indicators of amyloid burden in a population-based study of cognitively normal elderly. *Neurology* 79, 1570–1577.
- Morin, A., Michaud, J., 2007. Self-awareness and the left inferior frontal gyrus: inner speech use during self-related processing. *Brain Res. Bull.* 74, 387–396.
- Mormino, E.C., Brandel, M.G., Madison, C.M., Marks, S., Baker, S.L., Jagust, W.J., 2012. Abeta deposition in aging is associated with increases in brain activation during successful memory encoding. *Cereb. Cortex* 22, 1813–1823.
- Mosconi, L., Murray, J., Tsui, W.H., Li, Y., Spector, N., Goldowsky, A., Williams, S., Osorio, R., McHugh, P., Glodzik, L., Vallabhajosula, S., de Leon, M.J., 2014. Brain imaging of cognitively normal individuals with 2 parents affected by late-onset AD. *Neurology* 82, 752–760.
- Mosconi, L., Perani, D., Sorbi, S., Herholz, K., Nacmias, B., Holthoff, V., Salmon, E., Baron, J.C., De Cristofaro, M.T., Padovani, A., Borroni, B., Franceschi, M., Bracco, L., Pupi, A., 2004. MCI conversion to dementia and the APOE genotype: a prediction study with FDG-PET. *Neurology* 63, 2332–2340.
- Mosconi, L., Tsui, W.H., De Santi, S., Li, J., Rusinek, H., Convit, A., Li, Y., Boppana, M., de Leon, M.J., 2005. Reduced hippocampal metabolism in MCI and AD: automated FDG-PET image analysis. *Neurology* 64, 1860–1867.
- Mosconi, L., Tsui, W.H., Herholz, K., Pupi, A., Drzezga, A., Lucignani, G., Reiman, E.M., Holthoff, V., Kalbe, E., Sorbi, S., Diehl-Schmid, J., Perneczky, R., Clerici, F., Caselli, R., Beuthien-Baumann, B., Kurz, A., Minoshima, S., de Leon, M.J., 2008. Multicenter standardized 18F-FDG PET diagnosis of mild cognitive impairment, Alzheimer's disease, and other dementias. *J. Nucl. Med.* 49, 390–398.
- Mufson, E.J., Ma, S.Y., Cochran, E.J., Bennett, D.A., Beckett, L.A., Jaffar, S., Saragovi, H.U., Kordower, J.H., 2000. Loss of nucleus basalis neurons containing trkA immunoreactivity in individuals with mild cognitive impairment and early Alzheimer's disease. *J. Comp. Neurol.* 427, 19–30.
- Nakagawa, S., Cuthill, I.C., 2007. Effect size, confidence interval and statistical significance: a practical guide for biologists. *Biol. Rev. Camb. Philos. Soc.* 82, 591–605.
- Nestor, P.J., Fryer, T.D., Smielewski, P., Hodges, J.R., 2003. Limbic hypometabolism in Alzheimer's disease and mild cognitive impairment. *Ann. Neurol.* 54, 343–351.
- Nobili, F., Salmasso, D., Morbelli, S., Girtler, N., Piccardo, A., Brugnolo, A., Dessi, B., Larsson, S.A., Rodriguez, G., Pagani, M., 2008. Principal component analysis of FDG PET in amnesic MCI. *Eur. J. Nucl. Med. Mol. Imaging* 35, 2191–2202.
- Oh, H., Habeck, C., Madison, C., Jagust, W., 2014. Covarying alterations in Abeta deposition, glucose metabolism, and gray matter volume in cognitively normal elderly. *Hum. Brain Mapp.* 35, 297–308.
- Ostergaard, L., Aamand, R., Gutierrez-Jimenez, E., Ho, Y.C., Blicher, J.U., Madsen, S.M., Nagenthiraja, K., Dalby, R.B., Drasbek, K.R., Moller, A., Braendgaard, H., Mouridsen, K., Jespersen, S.N., Jensen, M.S., West, M.J., 2013. The capillary dysfunction hypothesis of Alzheimer's disease. *Neurobiol. Aging* 34, 1018–1031.
- Paulson, O.B., Hasselbalch, S.G., Rostrop, E., Knudsen, G.M., Pelligrino, D., 2010. Cerebral blood flow response to functional activation. *J. Cereb. Blood Flow Metab.* 30, 2–14.
- Peca, S., McCreary, C.R., Donaldson, E., Kumarpillai, G., Shobha, N., Sanchez, K., Charlton, A., Steinback, C.D., Beaudin, A.E., Fluck, D., Pillay, N., Fick, G.H., Poulin, M.J., Frayne, R., Goodyear, B.G., Smith, E.E., 2013. Neurovascular decoupling is associated with severity of cerebral amyloid angiopathy. *Neurology* 81, 1659–1665.
- Reiman, E.M., Chen, K., Alexander, G.E., Caselli, R.J., Bandy, D., Osborne, D., Saunders, A.M., Hardy, J., 2004. Functional brain abnormalities in young adults at genetic risk for late-onset Alzheimer's dementia. *Proc. Natl. Acad. Sci. U. S. A.* 101, 284–289.
- Riese, F., Gietl, A., Zolch, N., Henning, A., O'Gorman, R., Kalin, A.M., Leh, S.E., Buck, A., Warnock, G., Edden, R.A., Luechinger, R., Hock, C., Kollias, S., Michels, L., 2015. Posterior cingulate gamma-aminobutyric acid and glutamate/glutamine are reduced in amnesic mild cognitive impairment and are unrelated to amyloid deposition and apolipoprotein E genotype. *Neurobiol. Aging* 36, 53–59.
- Rostomian, A.H., Madison, C., Rabinovici, G.D., Jagust, W.J., 2011. Early 11C-PIB frames and 18F-FDG PET measures are comparable: a study validated in a cohort of AD and FTD patients. *J. Nucl. Med.* 52, 173–179.
- Scarmeas, N., Habeck, C.G., Stern, Y., Anderson, K.E., 2003. APOE genotype and cerebral blood flow in healthy young individuals. *JAMA* 290, 1581–1582.
- Scheff, S.W., Price, D.A., Schmitt, F.A., Scheff, M.A., Mufson, E.J., 2011. Synaptic loss in the inferior temporal gyrus in mild cognitive impairment and Alzheimer's disease. *J. Alzheimers Dis.* 24, 547–557.
- Schreiner, S.J., Liu, X., Gietl, A.F., Wyss, M., Steininger, S.C., Gruber, E., Treyer, V., Meier, I.B., Kalin, A.M., Leh, S.E., Buck, A., Nitsch, R.M., Pruessmann, K.P., Hock, C., Unschuld, P.G., 2014. Regional fluid-attenuated inversion recovery (FLAIR) at 7 Tesla correlates with amyloid beta in hippocampus and brainstem of cognitively normal elderly subjects. *Front. Aging Neurosci.* 6, 240.
- Solbach, C., Uebele, M., Reischl, G., Machulla, H.J., 2005. Efficient radiosynthesis of carbon-11 labelled uncharged Thioflavin T derivatives using [11C]methyl triflate for beta-amyloid imaging in Alzheimer's disease with PET. *Appl. Radiat. Isot.* 62, 591–595.
- Sperling, R.A., Aisen, P.S., Beckett, L.A., Bennett, D.A., Craft, S., Fagan, A.M., Ivatsubo, T., Jack Jr., C.R., Kaye, J., Montine, T.J., Park, D.C., Reiman, E.M., Rowe, C.C., Siemers, E., Stern, Y., Yaffe, K., Carrillo, M.C., Thies, B., Morrison-Bogorad, M., Wagster, M.V., Phelps, C.H., 2011. Toward defining the preclinical stages of Alzheimer's disease: recommendations from the National Institute on Aging-Alzheimer's Association workgroups on diagnostic guidelines for Alzheimer's disease. *Alzheimers Dement.* 7, 280–292.
- Sperling, R.A., Laviolette, P.S., O'Keefe, K., O'Brien, J., Rentz, D.M., Pihlajamaki, M., Marshall, G., Hyman, B.T., Selkoe, D.J., Hedden, T., Buckner, R.L., Becker, J.A., Johnson, K.A., 2009. Amyloid deposition is associated with impaired default network function in older persons without dementia. *Neuron* 63, 178–188.
- Steininger, S.C., Liu, X., Gietl, A., Wyss, M., Schreiner, S., Gruber, E., Treyer, V., Kalin, A., Leh, S., Buck, A., Nitsch, R.M., Prussmann, K.P., Hock, C., Unschuld, P.G., 2014. Cortical amyloid beta in cognitively normal elderly adults is associated with decreased network efficiency within the cerebro-cerebellar system. *Front. Aging Neurosci.* 6, 52.
- Takada, H., Nagata, K., Hirata, Y., Satoh, Y., Watahiki, Y., Sugawara, J., Yokoyama, E., Kondoh, Y., Shishido, F., Inugami, A., 1992. Age-related decline of cerebral oxygen metabolism in normal population detected with positron emission tomography. *Neurol. Res.* 14 (2 Suppl), 128–131.
- Thal, D.R., Griffin, W.S., de Vos, R.A., Ghebremedhin, E., 2008. Cerebral amyloid angiopathy and its relationship to Alzheimer's disease. *Acta Neuropathol.* 115, 599–609.
- Thambisetty, M., Beason-Held, L., An, Y., Kraut, M.A., Resnick, S.M., 2010. APOE epsilon4 genotype and longitudinal changes in cerebral blood flow in normal aging. *Arch. Neurol.* 67, 93–98.
- Vandenbergh, R., Van Laere, K., Ivanou, A., Salmon, E., Bastin, C., Triau, E., Hasselbalch, S., Law, I., Andersen, A., Korner, A., Minthon, L., Garraux, G., Nelissen, N., Bormans, G., Buckley, C., Owenius, R., Thurfjell, L., Farrar, G., Brooks, D.J., 2010. 18F-flutemetamol amyloid imaging in Alzheimer disease and mild cognitive impairment: a phase 2 trial. *Ann. Neurol.* 68, 319–329.
- Villemagne, V.L., Burnham, S., Bourgeat, P., Brown, B., Ellis, K.A., Salvado, O., Szoek, C., Macaulay, S.L., Martins, R., Maruff, P., Ames, D., Rowe, C.C., Masters, C.L., 2013. Amyloid beta deposition, neurodegeneration, and cognitive decline in sporadic Alzheimer's disease: a prospective cohort study. *Lancet Neurol.* 12, 357–367.
- Wierenga, C.E., Clark, L.R., Dev, S.I., Shin, D.D., Jurick, S.M., Rissman, R.A., Liu, T.T., Bondi, M.W., 2013. Interaction of age and APOE genotype on cerebral blood flow at rest. *J. Alzheimers Dis.* 34, 921–935.
- Winblad, B., Palmer, K., Kivipelto, M., Jelic, V., Fratiglioni, L., Wahlund, L.O., Nordberg, A., Backman, L., Albert, M., Almkvist, O., Arai, H., Basun, H., Blennow, K., de Leon, M., DeCarli, C., Erkinjuntti, T., Giacobini, E., Graff, C., Hardy, J., Jack, C., Jorm, A., Ritchie, K., van Duijn, C., Visser, P., Petersen, R.C., 2004. Mild cognitive impairment—beyond controversies, towards a consensus: report of the International Working Group on Mild Cognitive Impairment. *J. Intern. Med.* 256, 240–246.
- Zhang, S., Han, D., Tan, X., Feng, J., Guo, Y., Ding, Y., 2012. Diagnostic accuracy of 18 F-FDG and 11 C-PIB-PET for prediction of short-term conversion to Alzheimer's disease in subjects with mild cognitive impairment. *Int. J. Clin. Pract.* 66, 185–198.